JACS
JOURNAL OF THE AMERICAN CHEMICAL SOCIETY

pubs.acs.org/JACS

Article

Sequence-Specific Quantitation of Mutagenic DNA Damage via Polymerase Amplification with an Artificial Nucleotide

Claudia M. N. Aloisi, Arman Nilforoushan, Nathalie Ziegler, and Shana J. Sturla*

Cite This: J. Am. Chem. Soc. 2020, 142, 6962−6969

Read Online

ACCESS | Metrics & More | Article Recommendations | Supporting Information

ABSTRACT: DNA mutations can result from replication errors due to different forms of DNA damage, including low-abundance DNA adducts induced by reactions with electrophiles. The lack of strategies to measure DNA adducts within genomic loci, however, limits our understanding of chemical mutagenesis. The use of artificial nucleotides incorporated opposite DNA adducts by engineered DNA polymerases offers a potential basis for site-specific detection of DNA adducts, but the availability of effective artificial nucleotides that insert opposite DNA adducts is extremely limited, and furthermore, there has been no report of a quantitative strategy for determining how much DNA alkylation occurs in a sequence of interest. In this work, we synthesized an artificial nucleotide triphosphate that is selectively inserted opposite O^6-carboxymethyl-guanine DNA by an engineered polymerase and is required for DNA synthesis past the adduct. We characterized the mechanism of this enzymatic process and demonstrated that the artificial nucleotide is a marker for the presence and location in the genome of O^6-carboxymethyl-guanine. Finally, we established a mass spectrometric method for quantifying the incorporated artificial nucleotide and obtained a linear relationship with the amount of O^6-carboxymethyl-guanine in the target sequence. In this work, we present a strategy to identify, locate, and quantify a mutagenic DNA adduct, advancing tools for linking DNA alkylation to mutagenesis and for detecting DNA adducts in genes as potential diagnostic biomarkers for cancer prevention.

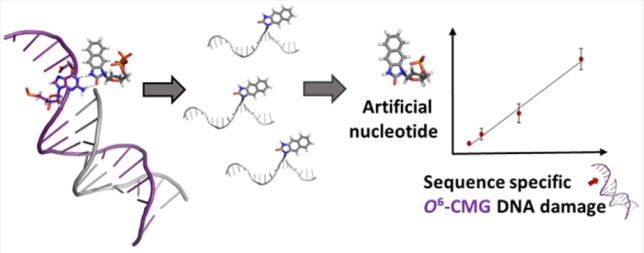

INTRODUCTION

DNA integrity is continuously threatened by endogenous and exogenous DNA-reactive chemicals. The resulting chemical adducts to DNA can initiate adverse biological consequences including cell death and mutation. O^6-Alkyl-guanines (O^6-alkylGs) are mutagenic DNA adducts that have been linked to carcinogenesis.[1−4] They can form from anticancer drugs,[5] antibiotics,[6] and environmental exposures such as cigarette smoke or red and processed meat consumption.[7−11] In particular, O^6-carboxymethyl-guanine (O^6-CMG; Figure 1B) was significantly higher in exfoliated colonocytes of people who eat meat vs vegetarians[10] and has been detected upon *in vitro* gastrointestinal digestion of meat,[11] suggesting its formation as a molecular initiating event in colorectal carcinogenesis (CRC) linked to meat consumption.[11−13]

Mutation spectra from colon cells of people with CRC resemble the spectrum induced by the carboxymethylating agent potassium diazoacetate (KDA).[14] Spectra measured in the cancer-relevant gene *p53* of CRC tissues and in a KDA-treated *p53* gene-containing plasmid were rich in C > T transition mutations, potentially arising from the misincorporation of T opposite O^6-CMG during replication, as suggested by *in vitro* studies interrogating the fidelity of replication past O^6-CMG.[15−17] When O^6-CMG was placed in a DNA template and replicated by translesion DNA synthesis (TLS) polymerases (Pols), it was found that O^6-CMG promotes the misincorporation of bases by Y- and B-family TLS Pols.[15] In another study, by transfecting a DNA plasmid containing O^6-CMG in human cells, it was concluded that O^6-CMG moderately blocks DNA replication and induces mutations at substantial frequencies.[16] While there is evidence regarding the mutagenic potential of O^6-CMG, there is however a lack of data concerning the presence and accumulation of O^6-CMG in CRC hotspot regions of the genome.

To establish a cause−effect relationship between O^6-CMG and CRC, the detection and quantification of DNA damage in the genome is critically needed. O^6-CMG is typically detected by P32 postlabeling,[18] immunoblotting,[19] affinity chromatography,[8] and mass spectrometry.[20−22] The most sensitive O^6-CMG measurement was by ESI-MS^3 with a LOQ of 73.4 amol,[22] allowing detection of 0.05 O^6-CMG per 10^7 nucleotides in human cells. However, for all approaches, only the total level of damage can be determined and information on the genomic location of O^6-CMG is lost.

Received: October 31, 2019
Published: March 20, 2020

https://dx.doi.org/10.1021/jacs.9b11746
J. Am. Chem. Soc. 2020, 142, 6962−6969

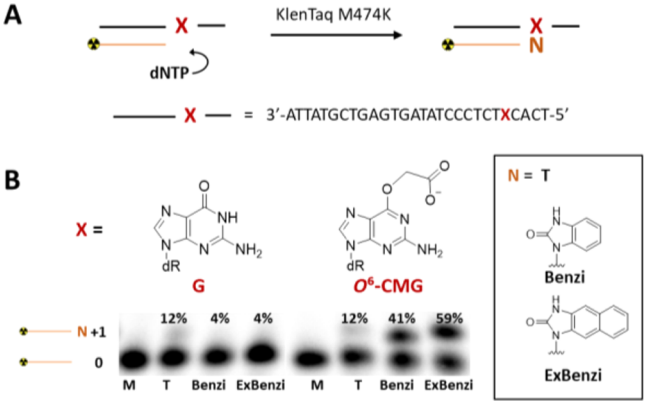

Figure 1. Single nucleotide incorporation opposite O^6-CMG. (A) Scheme of KlenTaq M747K-mediated single-nucleotide incorporation and DNA template sequence used in this study. (B) Single-nucleotide incorporation of T, Benzi, and ExBenzi opposite X = G or O^6-CMG, catalyzed by KlenTaq M747K, analyzed on denaturing polyacrylamide gels and visualized by autoradiography (M = marker lane with 23 nt primer).

A nanopore-based O^6-CMG sequencing approach has been recently applied to study the behavior of O^6-CMG during replication by Phi29 DNA Pol.[23] In this system, the presence of the adduct is associated with an alteration of current signal only for predefined arrangements of four-base contexts. Additionally, the characteristic signal was obtained by using a low-throughput nanopore that is not commercially available.

DNA adduct-directed artificial nucleotides have been developed as a basis for interrogating damaged DNA in duplex hybridization or polymerase-mediated synthesis contexts.[24] We have reported a variety of nucleoside analogues that stabilize damaged DNA vs undamaged DNA.[24−27] The heterocyclic imidic nucleoside analogue derived from benzimidazolinone (Benzi) and a derivative with an extended ρ-surface termed ExBenzi (Figure 1B) consist of a conjugated π-system, a hydrogen bond accepting carbonyl group, and an imino-based hydrogen bond donor. When placed opposite O^6-alkylG adducts, the resulting duplexes are stabilized.[27−31] When ExBenzi was included in short oligonucleotides attached to gold nanoparticles, the presence of O^6-alkylG adducts in target DNA strands disrupted nanoparticle aggregation and induced a color change, indicating the presence of the adduct.[28] These hybridization probes provide an excellent quantitative read-out, but do not involve DNA amplification and have so far been used to detect down to 138 fmol of modified DNA in 6 pmol of total DNA.

Polymerase-mediated amplification has revolutionized the life sciences, and the first report of its use to amplify a DNA adduct involved the bypass-proficient Pol mutant KlenTaq M747K[30−32] and the heterocyclic imidic nucleotide triphosphate (TP) Benzi. Benzi was selectively incorporated opposite O^6-alkylG, and DNA complementary to the damaged templates could be amplified by sequential repeats of primer extension reactions, with the presence of Benzi marking the damage location. However, the approach lacked any quantitative analysis capacity, meaning that the amount of O^6-alkylG in the DNA sample could not be determined.

To fulfill both the requirement of quantification of low-occurrence O^6-CMG and the need to retain information regarding the DNA sequence, we present herein a chemical−biochemical−analytical combined strategy for the quantitative detection of O^6-CMG in a sequence-targeted manner. We synthesized (Scheme S1) the triphosphate of the aromatic heterocyclic imide nucleoside ExBenzi and showed for the first time that it is specifically incorporated opposite O^6-CMG by an engineered Pol. We characterized the incorporation rates of ExBenziTP vs natural bases opposite O^6-CMG and used molecular modeling based on the KlenTaq M747K crystal structure to identify a structural basis for ExBenzi selectivity. Finally, we developed a mass spectrometric method to quantify the incorporated ExBenzi nucleoside, which reflects the amount of initial O^6-CMG. With this combination of chemical probe, polymerase-mediated synthesis, and mass spectrometric analysis, we were able to detect and quantify the O^6-CMG adduct in a specific DNA sequence context. With the capacity to target any DNA sequence, this strategy is anticipated to help elucidate how DNA damage in hotspot regions of the genome impact the mutagenesis and carcinogenesis processes.

RESULTS AND DISCUSSION

Artificial Nucleotide Analogue Is Incorporated Opposite the O^6-CMG DNA Adduct. To characterize the efficiency of incorporation of ExBenzi opposite O^6-CMG, we performed primer extension experiments using the engineered DNA Pol KlenTaq M747K, which has an established capacity to bypass and incorporate chemically modified nucleotides.[30−32] Thus, a 5′-end radiolabeled 23-nucleotide (nt) primer was annealed to a 28 nt template (SI, Material and Methods) with either G or O^6-CMG at nt position 24. The ability of KlenTaq M747K to incorporate ExBenzi opposite G or O^6-CMG was tested by incubating the annealed primer-template DNA with ExBenziTP and KlenTaq M747K at 55 °C for 10 min (Figure 1A). For comparison, the reaction was conducted with other single nucleotides as controls, i.e. the previously reported artificial nucleotide BenziTP and dTTP,

Table 1. Steady-State Kinetic Parameters for Nucleotide Incorporation by KlenTaq M747K DNA Polymerase

X*	dNTP	K_M [μM]	k_{cat} [min^{-1}]	k_{cat}/K_M [μM^{-1} min^{-1}]	relative[a] k_{cat}/K_M
O^6-CMG	C	689 ± 104	4.1	0.006	0.04
	T	196 ± 29	3.8	0.019	0.13
	Benzi	60 ± 14	3.7	0.062	0.44
	ExBenzi	48 ± 7	6.8	0.142	1
G	C	1.5 ± 0.2	26	17.5	123
	T	45 ± 7	2.2	0.048	0.34
	Benzi	32 ± 6	0.10	0.003	0.02
	ExBenzi	39 ± 5	0.14	0.003	0.02

[a]Relative k_{cat}/K_M equals catalytic efficiency (k_{cat}/K_M) relative to that of ExBenziTP incorporation opposite O^6-CMG

https://dx.doi.org/10.1021/jacs.9b11746
J. Am. Chem. Soc. 2020, 142, 6962−6969

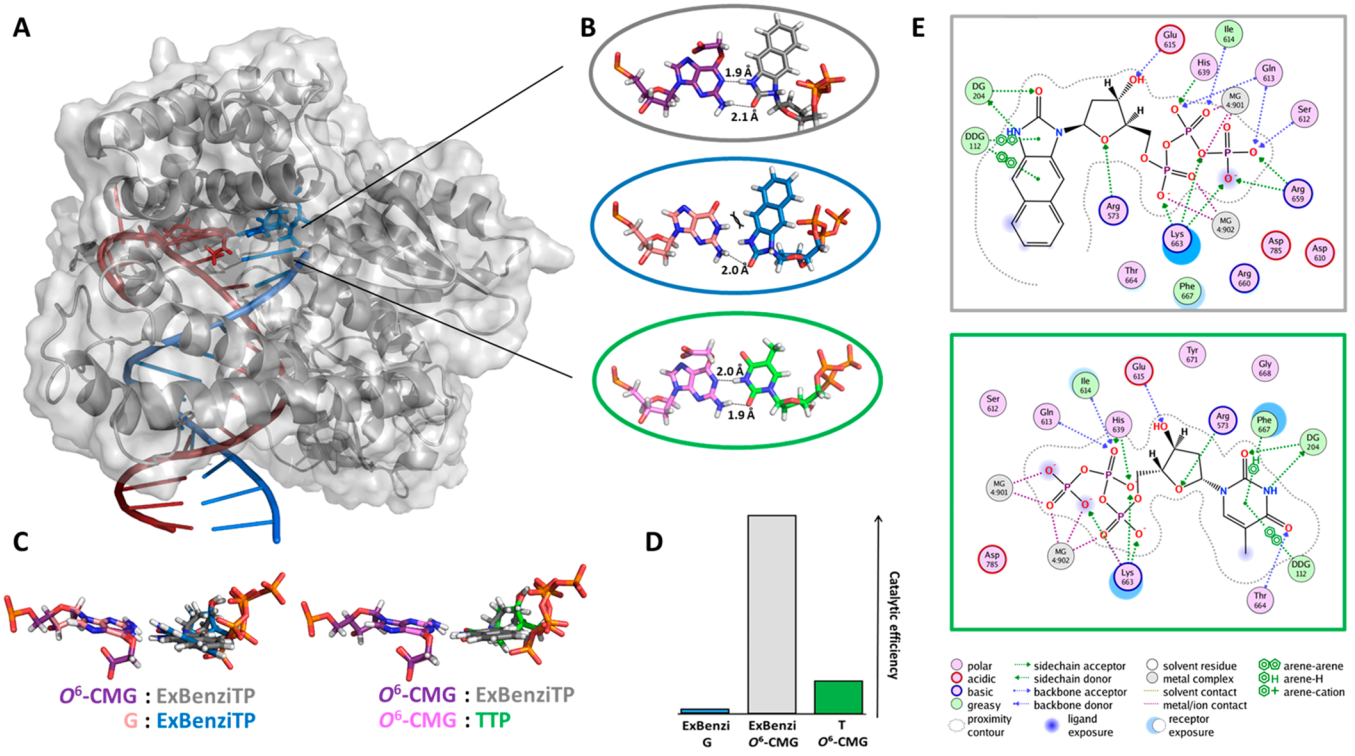

Figure 2. Molecular modeling of interactions in the active site of KlenTaq M747K. (A) KlenTaq M747K (PDB ID: 5O7T) was energy minimized with Molecular Operating Environment software. (B) In its active site (zoomed-in region), ExBenziTP paired opposite O^6-CMG (top) via two hydrogen bonds and opposite G (middle) via one hydrogen bond. dTTP paired opposite O^6-CMG (bottom) via two hydrogen bonds. (C) Overlay of base pairs O^6-CMG:ExBenziTP and O^6-CMG:TTP (similarly planarity, bottom). Opposite G, ExBenzi is tilted (top). (D) Relative catalytic efficiency (Table 1) of incorporation of ExBenziTP opposite G (blue bar) and opposite O^6-CMG (gray) and of TTP opposite O^6-CMG (green). (E) 2D ligand−protein interactions are shown between KlenTaq M747K and ExBenziTP (top) and TTP (bottom).

which is the canonical base most frequently incorporated opposite O^6-CMG by KlenTaq M747K.[30] The percentage of incorporated product was calculated as the ratio of the amount of n+1 extension product to the initial amount of primer (Figure 1B). We found that opposite O^6-CMG, ExBenzi is more efficiently incorporated (59%) than T (12%) and that it is incorporated at a higher level than the previously reported Benzi (41%). Opposite a template containing G, there was almost no evidence for nucleotide incorporation (4% for both Benzi and ExBenzi vs 12% for T).

To quantitatively assess the efficiencies of nucleotide incorporation and characterize how replication over O^6-CMG by KlenTaq M747K depends on the presence of ExBenziTP, steady-state kinetic analyses of these primer extension processes were performed. Thus, the amount of incorporation of single nucleotides was measured over time at increasing concentration of each nucleotide (Figure S2). Oligonucleotides resulting from single incorporation of nucleotides were separated on polyacrylamide gel and visualized by autoradiography. The equilibrium constant for binding affinity (K_M) and the catalytic turnover (k_{cat}) were derived for incorporation by KlenTaq M747K of Benzi, ExBenzi, T, or C, opposite G or O^6-CMG (Table 1). For ExBenzi incorporation, K_M values for incorporation templated by either damaged or undamaged DNA were very similar (48 and 39 μM, respectively). Interestingly, a higher binding affinity to the enzyme was calculated for ExBenzi and Benzi compared to T and to C (opposite O^6-CMG). Indeed, the K_M for insertion of ExBenzi opposite O^6-CMG was almost 4-fold lower than the K_M for insertion of T and 14-fold lower than the K_M for insertion of C (48, 196, and 689 μM, respectively). Conversely, k_{cat} for the incorporation of ExBenzi opposite O^6-CMG was almost 2-fold higher than for the incorporation of Benzi, T, or C in the same context. As a result, the catalytic efficiency (k_{cat}/K_M) for the incorporation of ExBenzi opposite O^6-CMG was 7- and 24-fold higher than for T or C, respectively, opposite O^6-CMG (Table 1). Remarkably, ExBenzi displayed the highest selectivity, almost 50-fold, for incorporation opposite damaged over undamaged DNA (Table 1; k_{cat}/K_M = 0.142 vs 0.003).

Structural Basis for ExBenziTP Selective Incorporation Opposite O^6-CMG by KlenTaq M747K. We were interested in understanding the physical basis for the highly selective incorporation of ExBenzi opposite O^6-CMG, despite its large size, both when compared to other nucleotides and in terms of template selectivity. Thus, we performed molecular modeling studies with ExBenziTP, BenziTP, or dTTP opposite O^6-CMG or G in DNA bound to KlenTaq M747K. Using a molecular mechanics-based computational modeling approach, we built a model starting from the crystal structure of KlenTaq M747K in a ternary complex with double-stranded DNA and an incoming dCTP (PDB ID: 5O7T). We then replaced incoming dCTP with ExBenziTP, BenziTP, or dTTP. The template strand had either G (original structure) or O^6-CMG opposite the incoming base. Upon energy minimization to identify the most stable and high-occupancy conformer of the constructed DNA−enzyme complex (Figure 2A), ExBenzi and O^6-CMG interacted by two hydrogen bonds (Figure 2B, top): one between the N1 of O^6-CMG and the −NH donor of ExBenzi (1.9 Å) and one between the NH_2 donor of O^6-CMG and the carbonyl group of ExBenzi (2.1 Å). These interactions

https://dx.doi.org/10.1021/jacs.9b11746
J. Am. Chem. Soc. 2020, 142, 6962−6969

are consistent with previous models[29,31] and crystallographic analysis[33] of a similar construct with Benzi. In contrast, the G:ExBenziTP structure predicted only one hydrogen bond (2.0 Å) and a potential steric clash between the −NH moiety on ExBenzi and the −NH at the N1 position on O^6-CMG (Figure 2B, middle), expected to hinder catalysis. As a result, the complex with O^6-CMG:ExBenziTP is predicted to be more stable (computed free energy of −8.0 kcal/mol) than that of G:ExBenziTP (+32.0 kcal/mol). Furthermore, by overlapping the above computed base pairs, we observed a different orientation for ExBenzi depending on whether it is paired with O^6-CMG or G (Figure 2C). When paired with G, the steric clash imposed a slight rotation to ExBenzi that resulted in reduced planarity. The computationally derived geometry and interactions of ExBenzi with O^6-CMG vs G help explain the experimentally derived catalytic parameters (Table 1 and graph in Figure 2D).

Having established a structural basis for template-selective incorporation of ExBenzi, we were interested in understanding the selective incorporation of ExBenziTP over TTP by KlenTaq M747K. Thus, we modeled O^6-CMG:TTP in the active site of the enzyme and found a similar planarity (Figure 2C) and hydrogen bond pattern (Figure 2B, bottom) for O^6-CMG:TTP and O^6-CMG:ExBenziTP, suggesting that in this instance interactions between the paired bases do not determine the selectivity of ExBenzi incorporation or that differences in the interactions are not evident in these models. We speculated that the interactions of the incoming base, ExBenziTP vs dTTP, with the enzyme might account for the highly favorable incorporation of ExBenzi over T opposite O^6-CMG, also based on the value of K_M calculated for ExBenziTP and dTTP incorporation, which suggests a stronger binding affinity for ExBenziTP (Table 1). Indeed, the energy calculated for the interaction of KlenTaq M747K with ExBenziTP is −225.2 kcal/mol vs −204.5 kcal/mol with dTTP. Interactions between the triphosphate groups of the incoming nucleotide and the enzyme made the largest contribution to this difference (Figure 2E). For example, when Arg659, predicted to interact strongly with the phosphate of ExBenziTP, was mutated to Ala, the computed energy difference was +43 kcal/mol, whereas when Phe667, predicted to interact with T base, was mutated to Ala, there was not a significant impact on computed energy (Figure S3). The interaction with the enzyme was predicted to be slightly more favorable for ExBenziTP when compared to BenziTP as well (not shown), in agreement with kinetic measurements (Table 1).

The modeling studies performed herein suggest that a combination of interactions of the incoming nucleotide with the polymerase and between the bases of the nascent pair drives the selective reaction. The interaction of an incoming base (e.g. TTP and ExBenziTP) with the enzyme represents a first energetic barrier in the incorporation process.[34] We speculate that, once in the active site, the interaction of the incoming TP with the templating base promotes the rate-limiting conformational changes of the enzyme required for insertion. Therefore, the stabilization of the system caused by the lowest-energy base pair is hypothesized to be pivotal in driving the base insertion (e.g. ExBenziTP opposite O^6-CMG vs G). Our findings provide a structural and energetic basis for the rational development of artificial nucleotides for DNA adduct detection and imply that the artificial nucleotides should be designed to compensate the altered hydrogen-bonding capacity of the DNA adduct and to favorably interact with the Pol enzyme responsible for DNA synthesis. Overall, modeling studies corroborated results of primer extension (Figure 1) and kinetics experiments (Table 1), supporting the further investigation of ExBenzi as a marker for O^6-CMG.

ExBenzi Is Required for Efficient Extension of a DNA Primer on a Damaged DNA Template. To test whether the polymerase can extend from ExBenzi once it is incorporated opposite O^6-CMG, we performed DNA primer extension studies under conditions suitable for synthesis of a full-length complement of the damaged DNA template. Reaction conditions were the same as for single nucleotide incorporation experiments, except that the reaction mixture was supplemented with all four natural dNTPs, with or without BenziTP or ExBenziTP (Figure 3A). Primer elongation products were

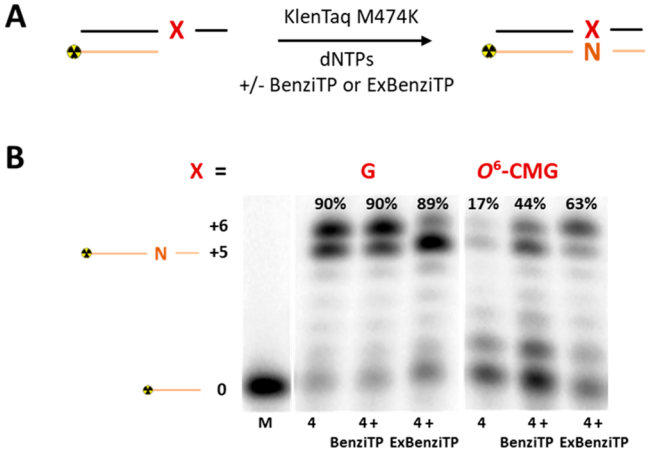

Figure 3. Primer extension past O^6-CMG. (A) Polymerase-mediated DNA synthesis. (B) Full extension of DNA primer complementary to undamaged (X = G) or damaged (X = O^6-CMG) DNA template, in the presence of all four natural dNTPS (4), and of BenziTP (4 + BenziTP) or of ExBenziTP (4 + ExBenziTP). Reactions were catalyzed by KlenTaq M747K for 10 min, analyzed on denaturing polyacrylamide gels, and visualized by autoradiography (M = marker lane with 23 nt primer).

analyzed on denaturing polyacrylamide gels and visualized by autoradiography. In the presence of all four natural dNTPs, replication was stalled at O^6-CMG, resulting in little (17%) fully extended primer. However, when either BenziTP or ExBenziTP was added, O^6-CMG was effectively bypassed (44% and 63% full-length products, respectively). Finally, we confirmed that replication of undamaged DNA (Figure 3B, X = G) in the presence of the four natural dNTPs occurs with full primer extension around 90% (band +5 and +6, Figure 3B), regardless of the presence of BenziTP or ExBenziTP. Thus, BenziTP and especially ExBenziTP promote full-length DNA synthesis past O^6-CMG, allowing replication of DNA containing O^6-CMG.

Having established ExBenzi as an effective complement to O^6-CMG, both when inserted and extended by KlenTaq M747K, we tested whether a primer annealed to a template containing O^6-CMG could be amplified in the presence of ExBenzi. For these studies, DNA primer and template were not preannealed: steps of annealing, primer extension, and duplex melting were repeated to allow the 28 nt DNA to template several rounds of primer extension. To maximize selectivity and enzyme efficiency, we optimized amplification cycles (Figure S4), temperature, and DNA and TP concentration

https://dx.doi.org/10.1021/jacs.9b11746
J. Am. Chem. Soc. 2020, 142, 6962−6969

(Figure S5). Optimal conditions consisted of 5 nM of 28 nt template, 300 nM of 23 nt primer, 10 μM of each dNTPs and of ExBenziTP, and 50 nM KlenTaq M747K (Figure 4A).

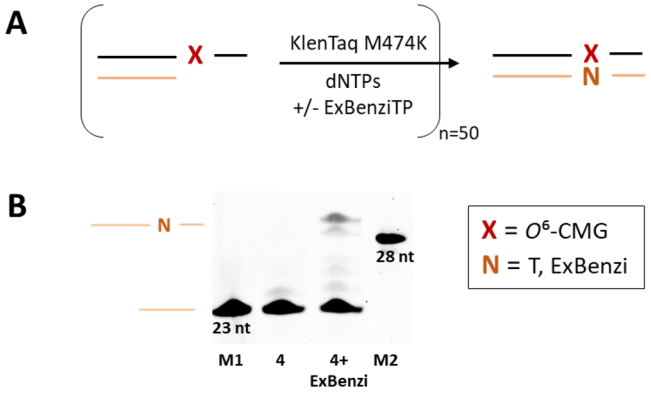

Figure 4. Reiterated DNA primer extension past O^6-CMG. (A) Scheme of cyclically repeated elongation past O^6-CMG. (B) Linear amplification of 6-FAM-labeled 23 nt primer and O^6-CMG 28 nt template in the presence or absence of ExBenziTP. Reactions were analyzed on denaturing polyacrylamide gels and visualized by fluorescence (M1 = marker lane with 23 nt primer; 4 = reaction with four natural dNTPs; 4 + ExBenzi = reaction with natural dNTPs + ExBenziTP; M2 = marker lane with 28 nt template, corresponding to the extended primer).

Alternating cycles (50) of DNA melting (95 °C, 30 s), annealing (42 °C, 30 s), and extension steps (55 °C, 30 s) were performed. Products were separated on a polyacrylamide gel and visualized by fluorescence (Figure 4B). Under these conditions, a signal for the full-length product was recorded only in the presence of ExBenziTP.

To assess whether the ExBenzi-promoted primer extension from damaged DNA could be applied to longer DNAs, we performed primer extension on a modified 4.7 kb plasmid. A 6-FAM-labeled 11 nt primer complementary to a region of the pEGFP-W plasmid preceding a G or O^6-CMG position was used (Figure S6A). In the presence of all four natural dNTPs, under fixed conditions (55 °C, 1 min extension, 50 nM KlenTaq M747K), the primer was extended up to around 200 bases when annealed to the unmodified plasmid, but not the O^6-CMG-modified plasmid (Figure S6B). When ExBenziTP also was added, however, the primer was effectively extended past O^6-CMG (Figure S6C), similar to what was observed with short oligonucleotides (Figure 4). Finally, longer products (>1 kb) could be obtained without affecting the selectivity by lengthening the elongation time to 4 min. These observations suggest the strategies characterized with oligonucleotide substrates have relevance for O^6-CMG in longer DNA samples.

These findings demonstrate that ExBenzi serves as a marker for the presence and location of O^6-CMG. It is required as a partner for replicating DNA past the adducts, up to around 200 bases. Furthermore, the amount of primer extended with oligonucleotide templates exceeded the initial amount of damaged template DNA present by roughly 18-fold, thereby increasing the potential signal from the amount of damage to the amount of marker probe. While these results support a biochemical basis for boosting the DNA damage signal, analyzing incorporation of ExBenziTP via gel assays limits the precision and sensitivity of quantifying DNA adducts, and coupled higher performance analytics strategies are needed.

Quantification of ExBenzi Nucleoside by Mass Spectrometry Is Diagnostic of O^6-CMG Levels in DNA. Having optimized the artificial nucleotide-engineered polymerase amplification strategy for O^6-CMG in a DNA sequence, we aimed to overcome limitations in quantifying O^6-CMG at low, difficult to detect amounts. Thus, we developed a mass spectrometric method for quantification of ExBenzi nucleoside from the amplicons. Linear amplification reactions in the presence of all four natural nucleotides and ExBenziTP were performed using either O^6-CMG DNA or unmodified DNA as template, analogous to that described in the previous paragraph. Amplified DNA was enzymatically hydrolyzed to nucleosides and purified for mass spectrometric analysis.

ExBenzi nucleoside was quantified by LC-MS/MS in SRM mode, by monitoring the transition m/z 301 → 185 (Figure S7). To correct for normal instrument variation and account for sample loss during processing, we evaluated artificial nucleosides that are structural analogues of ExBenzi, such as Benzi, the perimidinone Per, and the benzimidazole derivatives BIM and ExBIM, as internal standards (IS) that could avoid the need for synthesizing isotopically modified ExBenzi.[28−31] ExBIM nucleoside was optimal in having similar chemical properties to ExBenzi nucleoside, eluting at a similar retention time, and having a unique mass transition of m/z 285 → 169. We optimized the preparation of samples to achieve a similar recovery for ExBenzi nucleoside and for the IS ExBIM nucleoside of 90%.

To quantify the ExBenzi nucleoside, calibration curves were prepared (Figure S7) in the presence of sample matrix, consisting of nucleosides, enzyme, and salts (1xKTQ, SI), as a matrix effect was observed for the ionization of both nucleosides. Standard samples in matrix were prepared analogously to what was described above for the experimental samples. Briefly, linear amplification reactions were run using an unmodified DNA template under the usual conditions but in the absence of ExBenzi. Samples were spiked with IS ExBIM (10 nM) and with ExBenzi (5−500 nM). By relating the signal of ExBenzi to that of ExBIM, we could quantify ExBenzi nucleoside in a matrix with a LOQ of 20 fmol (Figure S7). Analysis of ExBenzi released from amplicons that were templated with DNA containing O^6-CMG showed a linear increase of ExBenzi signal with increasing concentrations of O^6-CMG in the template. ExBenzi could be detected also when reactions were performed with unmodified DNA, probably due to unspecific incorporation or noncovalent binding of ExBenzi, such as intercalation.[35] We could reduce the unspecific signal by disrupting such noncovalent interactions by varying pH or salt concentration; however, these additional sample processing steps significantly reduced recovery rates. Therefore, the background levels of ExBenzi in samples arising from amplification of unmodified DNA was used for background subtraction for the analysis. Thus, we found a linear increase of ExBenzi with increasing initial O^6-CMG levels in the template (Figure 5).

The approach described here establishes for the first time a chemical basis for amplification and quantitation of DNA damage in a sequence-targeted manner. This approach is useful for the study of isolated oligonucleotides or longer DNA; however, the sensitivity is insufficient for sequence-specific adduct detection of samples from cells. In cultured cells exposed to azaserine (0−450 μM), O^6-CMG levels were 0.3−9.1 lesions/10^7 nucleotides.[22] The low occurrence of O^6-CMG is even more relevant in the case of sequence-specific

https://dx.doi.org/10.1021/jacs.9b11746
J. Am. Chem. Soc. 2020, 142, 6962−6969

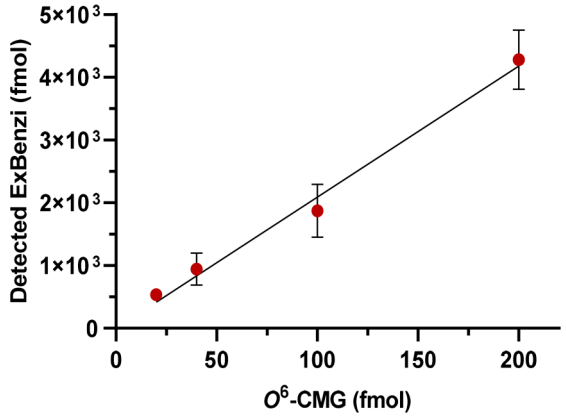

Figure 5. Quantitation of ExBenzi in amplicons from DNA containing O^6-CMG. ExBenzi incorporated by linearly amplified primer reactions from DNA with varying amounts of O^6-CMG by mass spectrometry, based on the calibration curve in Figure S8. Data are the average from four independent replicates, each made of two technical replicates. R^2 = 0.95.

detection; for example, there are only 5 guanines per genome (i.e. 6.6×10^9 nucleotides) belonging to codons 12 and 13 of the *k-ras* gene, which are commonly mutated in CRC.[36] With the combined strategy described here, assuming all *k-ras* Gs are carboxymethylated, an increase of sensitivity of a few orders of magnitude is needed. Nonetheless, for cell-based applications, there are several aspects that can be developed in future studies to address this limitation, including polymerase enzyme engineering/evolution,[37−39] higher mass spectrometric sensitivity, and sample enrichment.[40]

Bypass of O^6-MeG Occurs Independent of ExBenzi. In addition to the hurdle of extremely low abundance of DNA adducts in cells, other adducts form, mostly O^6-MeG, under related conditions.[7−11] Since ExBenzi also can be incorporated opposite O^6-MeG, and potentially unrelated adducts from different sources, the presence of O^6-MeG in biological samples by the approach described here could lead to overestimation of O^6-CMG. Incorporation rates opposite O^6-MeG are generally higher than O^6-CMG (6-fold increase for T and ExBenzi; Table S1). Despite this, an integral selection feature of the O^6-CMG-targeting approach is that DNA synthesis past O^6-CMG by KlenTaq M747K is low in the presence of natural dNTPs, requiring ExBenzi for extension, whereas O^6-MeG is readily extended in the absence of ExBenzi (Figure S1B), due to the high incorporation of T (Figure S1A). Therefore, the combination of ExBenziTP and KlenTaq M747K is a poor indicator of O^6-MeG levels, and these observations are consistent with those previously reported for Benzi.[31] Nevertheless, further approaches may be envisioned, such as extending preannealed primers first in the absence of ExBenziTP, resulting mainly in the extension of primer annealed to O^6-MeG, then adding ExBenziTP to extend past O^6-CMG targets (Figure S1C). Future work will be focused on characterizing chemical and biochemical aspects that drive adduct−triphosphate interactions and on targeting structural and enzymatic features to enable complementary strategies that address diverse adducts in heterogeneous biological samples.

CONCLUSION

Interest in understanding the genomic location of DNA adducts is growing in medical sciences,[41−45] due to causative links to mutagenicity and carcinogenesis,[46] as well as drug efficacy.[47] The O^6-CMG DNA adduct focused on in this study is mutagenic and hypothesized to be linked with CRC development.[11−13] We developed a strategy combining sequence-specific extension, increase in copy number of marker strands, and quantitation of a unique synthetic nucleoside as a reporter of levels of O^6-CMG DNA adducts in a DNA oligonucleotide. The artificial synthetic nucleotide ExBenzi is the most specifically and efficiently incorporated opposite O^6-CMG reported to date. We elucidated a structural basis for the high selectivity and specificity involving complementarity of H bonds and planarity of the O^6-CMG:ExBenziTP pair in the KlenTaq M747K active site. Finally, we developed a mass spectrometric method for quantification of ExBenzi nucleoside and showed that the amount of ExBenzi incorporated during DNA synthesis correlates linearly with the initial O^6-CMG DNA, allowing therefore its quantitation. The detection of O^6-CMG with retention of DNA sequence information presented in this study lays a foundation to address relationships between DNA damage and mutations in hotspot regions of the genome needed for predictive or prediagnostic purposes.

ASSOCIATED CONTENT

Supporting Information

The Supporting Information is available free of charge at https://pubs.acs.org/doi/10.1021/jacs.9b11746.

Material and methods, characterization data for synthetic triphosphate, supplementary Figures S1−S8, and corresponding references (PDF)

AUTHOR INFORMATION

Corresponding Author

Shana J. Sturla − *Department of Health Sciences and Technology, ETH Zürich 8092 Zurich, Switzerland;* orcid.org/0000-0001-6808-5950; Email: sturlas@ethz.ch

Authors

Claudia M. N. Aloisi − *Department of Health Sciences and Technology, ETH Zürich 8092 Zurich, Switzerland;* orcid.org/0000-0002-2279-7757

Arman Nilforoushan − *Department of Health Sciences and Technology, ETH Zürich 8092 Zurich, Switzerland*

Nathalie Ziegler − *Department of Health Sciences and Technology, ETH Zürich 8092 Zurich, Switzerland;* orcid.org/0000-0003-1152-0645

Complete contact information is available at: https://pubs.acs.org/10.1021/jacs.9b11746

Notes

The authors declare no competing financial interest.

ACKNOWLEDGMENTS

The research was supported by the Swiss National Science Foundation (156280, 185020) and the European Research Council (260341). We are very grateful to Emma Sandell (ETH Zurich) for so promptly and kindly sharing DNA plasmid.

REFERENCES

(1) Du, H.; Wang, P.; Li, L.; Wang, Y. Repair and translesion synthesis of O^6-alkylguanine DNA lesions in human cells. *J. Biol. Chem.* **2019**, *294* (29), 11144−11153.

(2) Ezerskyte, M.; Paredes, J. A.; Malvezzi, S.; Burns, J. A.; Margison, G. P.; Olsson, M.; Scicchitano, D. A.; Dreij, K. O^6-methylguanine-induced transcriptional mutagenesis reduces p53 tumor-suppressor function. *Proc. Natl. Acad. Sci. U. S. A.* **2018**, *115* (18), 4731−4736.

(3) Wang, P.; Wang, Y. Cytotoxic and mutagenic properties of O^6-alkyl-2′-deoxyguanosine lesions in Escherichia coli cells. *J. Biol. Chem.* **2018**, *293* (39), 15033−15042.

(4) Margison, G. P.; Santibanez Koref, M. F.; Povey, A. C. Mechanisms of carcinogenicity/chemotherapy by O^6-methylguanine. *Mutagenesis* **2002**, *17* (6), 483−7.

(5) Roos, W. P.; Batista, L. F.; Naumann, S. C.; Wick, W.; Weller, M.; Menck, C. F.; Kaina, B. Apoptosis in malignant glioma cells triggered by the Temozolomide-induced DNA lesion O^6-methylguanine. *Oncogene* **2007**, *26* (2), 186−97.

(6) Bennett, R. A.; Pegg, A. E. Alkylation of DNA in rat tissues following administration of streptozotocin. *Cancer Res.* **1981**, *41* (7), 2786−90.

(7) Montesano, R. Alkylation of DNA and tissue specificity in nitrosamine carcinogenesis. *J. Supramol. Struct. Cell. Biochem.* **1981**, *17* (3), 259−73.

(8) Harrison, K. L.; Jukes, R.; Cooper, D. P.; Shuker, D. E. Detection of concomitant formation of O^6-carboxymethyl- and O^6-methyl-2′-deoxyguanosine in DNA exposed to nitrosated glycine derivatives using a combined immunoaffinity/HPLC method. *Chem. Res. Toxicol.* **1999**, *12* (1), 106−11.

(9) Vanden Bussche, J.; Hemeryck, L. Y.; Van Hecke, T.; Kuhnle, G. G.; Pasmans, F.; Moore, S. A.; Van de Wiele, T.; De Smet, S.; Vanhaecke, L. O^6-carboxymethylguanine DNA adduct formation and lipid peroxidation upon in vitro gastrointestinal digestion of haem-rich meat. *Mol. Nutr. Food Res.* **2014**, *58* (9), 1883−96.

(10) Lewin, M. H.; Bailey, N.; Bandaletova, T.; Bowman, R.; Cross, A. J.; Pollock, J.; Shuker, D. E.; Bingham, S. A. Red meat enhances the colonic formation of the DNA adduct O^6-carboxymethyl guanine: implications for colorectal cancer risk. *Cancer Res.* **2006**, *66* (3), 1859−65.

(11) Hemeryck, L. Y.; Rombouts, C.; Hecke, T. V.; Van Meulebroek, L.; Bussche, J. V.; De Smet, S.; Vanhaecke, L. In vitro DNA adduct profiling to mechanistically link red meat consumption to colon cancer promotion. *Toxicol. Res.* **2016**, *5* (5), 1346−1358.

(12) Cross, A. J.; Ferrucci, L. M.; Risch, A.; Graubard, B. I.; Ward, M. H.; Park, Y.; Hollenbeck, A. R.; Schatzkin, A.; Sinha, R. A large prospective study of meat consumption and colorectal cancer risk: an investigation of potential mechanisms underlying this association. *Cancer Res.* **2010**, *70* (6), 2406−14.

(13) Steinberg, P. Red Meat-Derived Nitroso Compounds, Lipid Peroxidation Products and Colorectal Cancer. *Foods* **2019**, *8* (7), 252.

(14) Gottschalg, E.; Scott, G. B.; Burns, P. A.; Shuker, D. E. Potassium diazoacetate-induced p53 mutations in vitro in relation to formation of O^6-carboxymethyl- and O^6-methyl-2′-deoxyguanosine DNA adducts: relevance for gastrointestinal cancer. *Carcinogenesis* **2006**, *28* (2), 356−62.

(15) Raz, M. H.; Dexter, H. R.; Millington, C. L.; van Loon, B.; Williams, D. M.; Sturla, S. J. Bypass of Mutagenic O^6-Carboxymethylguanine DNA Adducts by Human Y- and B-Family Polymerases. *Chem. Res. Toxicol.* **2016**, *29* (9), 1493−503.

(16) Wu, J.; Wang, P.; Li, L.; Williams, N. L.; Ji, D.; Zahurancik, W. J.; You, C.; Wang, J.; Suo, Z.; Wang, Y. Replication studies of carboxymethylated DNA lesions in human cells. *Nucleic Acids Res.* **2017**, *45* (12), 7276−7284.

(17) Raz, M. H.; Sandell, E. S.; Patil, K. M.; Gillingham, D. G.; Sturla, S. J. High Sensitivity of Human Translesion DNA Synthesis Polymerase kappa to Variation in O^6-Carboxymethylguanine Structures. *ACS Chem. Biol.* **2019**, *14* (2), 214−222.

(18) Terasaki, M.; Totsuka, Y.; Nishimura, K.; Mukaisho, K.; Chen, K. H.; Hattori, T.; Takamura-Enya, T.; Sugimura, T.; Wakabayashi, K. Detection of endogenous DNA adducts, O-carboxymethyl-2′-deoxyguanosine and 3-ethanesulfonic acid-2′-deoxycytidine, in the rat stomach after duodenal reflux. *Cancer Sci.* **2008**, *99* (9), 1741−6.

(19) Cupid, B. C.; Zeng, Z.; Singh, R.; Shuker, D. E. Detection of O^6-carboxymethyl-2′-deoxyguanosine in DNA following reaction of nitric oxide with glycine and in human blood DNA using a quantitative immunoslot blot assay. *Chem. Res. Toxicol.* **2004**, *17* (3), 294−300.

(20) Vanden Bussche, J.; Moore, S. A.; Pasmans, F.; Kuhnle, G. G.; Vanhaecke, L. An approach based on ultra-high pressure liquid chromatography-tandem mass spectrometry to quantify O^6-methyl and O^6-carboxymethylguanine DNA adducts in intestinal cell lines. *J. Chromatogr A* **2012**, *1257*, 25−33.

(21) Da Pieve, C.; Sahgal, N.; Moore, S. A.; Velasco-Garcia, M. N. Development of a liquid chromatography/tandem mass spectrometry method to investigate the presence of biomarkers of DNA damage in urine related to red meat consumption and risk of colorectal cancer. *Rapid Commun. Mass Spectrom.* **2013**, *27* (21), 2493−503.

(22) Yu, Y.; Wang, J.; Wang, P.; Wang, Y. Quantification of Azaserine-Induced Carboxymethylated and Methylated DNA Lesions in Cells by Nanoflow Liquid Chromatography-Nanoelectrospray Ionization Tandem Mass Spectrometry Coupled with the Stable Isotope-Dilution Method. *Anal. Chem.* **2016**, *88* (16), 8036−42.

(23) Wang, Y. P.; Kiran, M.; Yan, S.; Zhang, P.; Guo, W.; Wang, Y.; Chen, H.-Y.; Gillingham, D.; Huang, S. Nanopore Sequencing Accurately Identifies the Mutagenic DNA Lesion O^6-Carboxymethyl Guanine and Reveals Its Behavior in Replication. *Angew. Chem., Int. Ed.* **2019**, *58* (25), 8432−8436.

(24) Raz, M. H.; Aloisi, C. M. N.; Gahlon, H. L.; Sturla, S. J. DNA Adduct-Directed Synthetic Nucleosides. *Acc. Chem. Res.* **2019**, *52* (5), 1391−1399.

(25) Gong, J.; Sturla, S. J. A synthetic nucleoside probe that discerns a DNA adduct from unmodified DNA. *J. Am. Chem. Soc.* **2007**, *129* (16), 4882−3.

(26) Gahlon, H. L.; Sturla, S. J. Hydrogen bonding or stacking interactions in differentiating duplex stability in oligonucleotides containing synthetic nucleoside probes for alkylated DNA. *Chem. - Eur. J.* **2013**, *19* (33), 11062−7.

(27) Dahlmann, H. D.; Berger, F. D.; Kung, R. W.; Wyss, L. A.; Gubler, I.; McKeague, M.; Wetmore, S. D.; Sturla, S. J., Fluorescent Nucleobase Analogues with Extended Pi Surfaces Stabilize DNA Duplexes Containing O^6-Alkylguanine Adducts. *Helv. Chim. Acta* **2018**, *7* (101), e1800066.

(28) Trantakis, I. A.; Nilforoushan, A.; Dahlmann, H. A.; Stauble, C. K.; Sturla, S. J. In-Gene Quantification of O^6-Methylguanine with Elongated Nucleoside Analogues on Gold Nanoprobes. *J. Am. Chem. Soc.* **2016**, *138* (27), 8497−504.

(29) Aloisi, C. M. N.; Sturla, S. J.; Gahlon, H. L. A gene-targeted polymerase-mediated strategy to identify O^6-methylguanine damage. *Chem. Commun.* **2019**, *55* (27), 3895−3898.

(30) Wyss, L. A.; Nilforoushan, A.; Eichenseher, F.; Suter, U.; Blatter, N.; Marx, A.; Sturla, S. J. Specific incorporation of an artificial nucleotide opposite a mutagenic DNA adduct by a DNA polymerase. *J. Am. Chem. Soc.* **2015**, *137* (1), 30−3.

(31) Wyss, L. A.; Nilforoushan, A.; Williams, D. M.; Marx, A.; Sturla, S. J. The use of an artificial nucleotide for polymerase-based recognition of carcinogenic O^6-alkylguanine DNA adducts. *Nucleic Acids Res.* **2016**, *44* (14), 6564−73.

(32) Gloeckner, C.; Sauter, K. B.; Marx, A. Evolving a thermostable DNA polymerase that amplifies from highly damaged templates. *Angew. Chem., Int. Ed.* **2007**, *46* (17), 3115−7.

(33) Betz, K.; Nilforoushan, A.; Wyss, L. A.; Diederichs, K.; Sturla, S. J.; Marx, A. Structural basis for the selective incorporation of an artificial nucleotide opposite a DNA adduct by a DNA polymerase. *Chem. Commun.* **2017**, *53* (94), 12704−12707.

(34) Hubscher, U. *DNA Polymerases: Discovery, Characterization, and Functions in Cellular DNA Transactions*; World Scientific, 2010 DOI: 10.1142/7667.

https://dx.doi.org/10.1021/jacs.9b11746
J. Am. Chem. Soc. 2020, 142, 6962−6969

(35) Kowal, E. A.; Lad, R. R.; Pallan, P. S.; Dhummakupt, E.; Wawrzak, Z.; Egli, M.; Sturla, S. J.; Stone, M. P. Recognition of O^6-benzyl-2′-deoxyguanosine by a perimidinone-derived synthetic nucleoside: a DNA interstrand stacking interaction. *Nucleic Acids Res.* **2013**, *41* (15), 7566−76.
(36) Yoon, H. H.; Tougeron, D.; Shi, Q.; Alberts, S. R.; Mahoney, M. R.; Nelson, G. D.; Nair, S. G.; Thibodeau, S. N.; Goldberg, R. M.; Sargent, D. J.; Sinicrope, F. A. KRAS codon 12 and 13 mutations in relation to disease-free survival in BRAF-wild-type stage III colon cancers from an adjuvant chemotherapy trial (N0147 alliance). *Clin. Cancer Res.* **2014**, *20* (11), 3033−43.
(37) Gloeckner, C.; Kranaster, R.; Marx, A. Directed evolution of DNA polymerases: construction and screening of DNA polymerase mutant libraries. *Curr. Protoc Chem. Biol.* **2010**, *2* (2), 89−109.
(38) Wang, Y.; Ngor, A. K.; Nikoomanzar, A.; Chaput, J. C. Evolution of a General RNA-Cleaving FANA Enzyme. *Nat. Commun.* **2018**, *9* (1), 5067.
(39) Tretyakova, N.; Goggin, M.; Sangaraju, D.; Janis, G. Quantitation of DNA adducts by stable isotope dilution mass spectrometry. *Chem. Res. Toxicol.* **2012**, *25* (10), 2007−35.
(40) Szychowski, J.; Mahdavi, A.; Hodas, J. J.; Bagert, J. D.; Ngo, J. T.; Landgraf, P.; Dieterich, D. C.; Schuman, E. M.; Tirrell, D. A. Cleavable biotin probes for labeling of biomolecules via azide-alkyne cycloaddition. *J. Am. Chem. Soc.* **2010**, *132* (51), 18351−60.
(41) Sloan, D. B.; Broz, A. K.; Sharbrough, J.; Wu, Z. Detecting Rare Mutations and DNA Damage with Sequencing-Based Methods. *Trends Biotechnol.* **2018**, *36* (7), 729−740.
(42) Wu, J.; McKeague, M.; Sturla, S. J. Nucleotide-Resolution Genome-Wide Mapping of Oxidative DNA Damage by Click-Code-Seq. *J. Am. Chem. Soc.* **2018**, *140* (31), 9783−9787.
(43) Hu, J.; Adebali, O.; Adar, S.; Sancar, A. Dynamic maps of UV damage formation and repair for the human genome. *Proc. Natl. Acad. Sci. U. S. A.* **2017**, *114* (26), 6758−6763.
(44) Shu, X.; Xiong, X.; Song, J.; He, C.; Yi, C. Base-Resolution Analysis of Cisplatin-DNA Adducts at the Genome Scale. *Angew. Chem., Int. Ed.* **2016**, *55* (46), 14246−14249.
(45) Li, W.; Hu, J.; Adebali, O.; Adar, S.; Yang, Y.; Chiou, Y. Y.; Sancar, A. Human genome-wide repair map of DNA damage caused by the cigarette smoke carcinogen benzo[a]pyrene. *Proc. Natl. Acad. Sci. U. S. A.* **2017**, *114* (26), 6752−6757.
(46) Basu, A. K.; Nohmi, T. Chemically-Induced DNA Damage, Mutagenesis, and Cancer. *Int. J. Mol. Sci.* **2018**, *19* (6), 1767.
(47) Stornetta, A.; Zimmermann, M.; Cimino, G. D.; Henderson, P. T.; Sturla, S. J. DNA Adducts from Anticancer Drugs as Candidate Predictive Markers for Precision Medicine. *Chem. Res. Toxicol.* **2017**, *30* (1), 388−409.

https://dx.doi.org/10.1021/jacs.9b11746
J. Am. Chem. Soc. 2020, 142, 6962−6969